

## Micro-Ball Wafer Bumping for Flip Chip Interconnection

Eiji Hashino, Kenji Shimokawa, Yukihiko Yamamoto and Kohei Tatsumi  
Nippon Steel Corporation, Advanced Technology Research Laboratories  
20-1 Shintomi, Futtsu, Chiba 293-8511 Japan  
TEL: 81-439-80-2879 FAX: 81-439-80-2746 e-mail: hashino@re.nsc.co.jp

### Abstract

A new wafer bumping method using micro-balls was developed that can be used for high-density LSI assembly, specifically for Flip Chip interconnection. Micro solder balls with the diameter ranging from 60  $\mu\text{m}$  to 200  $\mu\text{m}$  were first formed with a high level of accuracy and sphericity. These balls were transferred and bonded to the whole electrode-pads of an 8-inch wafer in one stroke using a fully automated micro ball moulder, which was newly developed. The balls were held on fluxed pads and melted in a reflow furnace. The fluxing was performed using unique stamp system. The productivity and the yield were evaluated under the following conditions. The number of chips on an 8 inch wafer was 616, Pad pitch was 250  $\mu\text{m}$ , Pad number of a chip was 625 (25x25 area array), and the total number of balls on a wafer was 385,000. The yield of forming bumps was confirmed to be higher than 99.995% without repairing and the cycle time of micro ball bumping was ca. 5 min. for an 8 inch wafer. The bump height variation, the bump shear strength and the bond reliability were evaluated in comparison with other methods.

### Introduction

The technology of connecting semiconductor chip electrode pads to lead frames with bonding wires finds plenty of field-proven records, attesting to the high level of reliability. This wire bonding technology, therefore, has so far been widely used due to the good bonding quality as well as the flexibility of packaging design. The wiring length, however, sometimes poses a problem as the level of density is further increasing and high-speed devices are required to deliver even greater high-frequency performance. In this situation, part of the chip interconnection technologies using bonding wires is being replaced by the TAB and Flip Chip interconnection technologies of forming bumps on chips and bonding chips via these bumps. Especially FC is the most suitable for the needs.

Since the introduction of the Flip Chip technology by IBM in the 1960s, various Flip Chip bumping technologies have been intensively investigated particularly in the past decade as superior high-density packaging technologies capable of delivering much better electrical performance and a high level of manufacturability than the wire bonding technique [1]-[3]. A typical bumping technology in use today allows the UBM to be first formed in aluminum electrode pads and then solder bumps to be formed in the position of electrode pads on a wafer using shadow masks or photo-resist by means of physical vapor deposition (PVD), such as evaporation and sputtering. Although this vapor deposition process has proven track records with respect of its reliability, a large vacuum



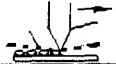

chamber and photo-masks are required and consequently the cost becomes high. In addition, it is pointed out that the majority of vapor-evaporated metals are not used as bumps and eventually become wastes.

Studies in the technology of forming solder bumps using the plating process have progressed to a stage where they can currently achieve commercial viability. Some drawbacks, however, are pointed out: complex process, environment-related problems that must be resolved, and the freedom of alloy plating composition selectivity small. Although the current main alloy composition that is used is Pb-Sn alloy, it is anticipated that the use of Pb is restricted for the reason of environment-related problems, indicating the need to use various types of Pb-free alloy solder.

The method of forming solder bumps by stencil printing or screen-printing the solder paste is recently being made practical. It is understood that this method has the advantage of greater throughput and superior solder material selectivity but is not suitable for the fine pitch bumping operation [3].

This paper describes a new technique for forming Flip Chip bumps on a wafer, featuring the formation of micro-balls with a high level of precision and sphericity. Using this technique, bumps can be formed with high precision and efficiency and, at the same time, much greater flexibility in the selection of bump metals becomes possible. The comparison of each forming method is shown in Table 1.

Table 1. Comparison of bumping methods for Flip Chip.

	Advantage	Disadvantage
Evaporation 	Proven technology	Complex process High material waste Alloy control difficult
Plating 	Proven technology Fine pitch	Many steps Alloy control difficult Environmental
Paste printing 	High throughput Solder paste process	Not fine pitch Bump height distribution
Micro-ball bumping 	High throughput Uniform bump height Flexible alloy selection	New technology Tooling required

### Micro-Ball Preparation

Various Pb-Sn alloys, Pb free solder materials and other metals of relatively high melting points can be used as the bump material. The ball material in solid form is cut into units of specified mass that are heated and melted at temperature well higher than the material's melting point and made into balls. The surface tension of liquid metal function to produce balls those make a high level of sphericity. After considering the melting point and oxidation characteristics of the material to be melted, the most appropriate atmosphere, such as, a vacuum atmosphere, a gaseous atmosphere or a reducing atmosphere is selected. The height and pitch of bumps to be formed on electrode pads are considered to determine the size of balls.

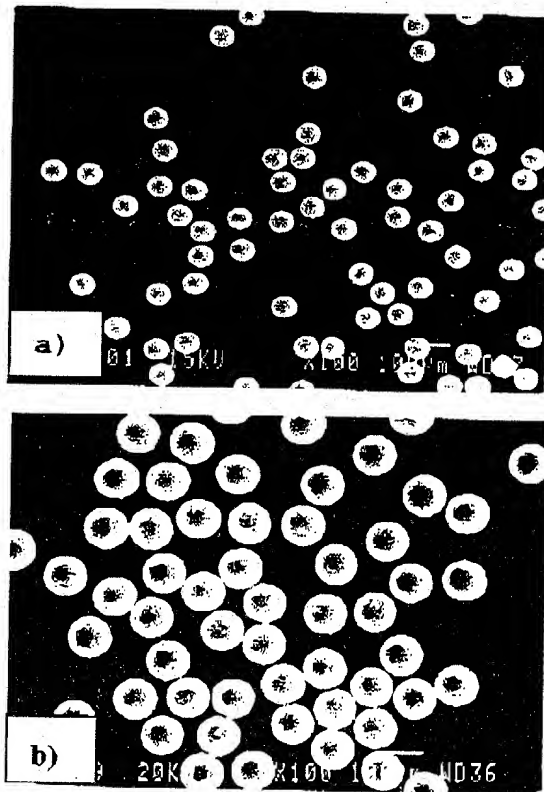


Figure 1. SEM images of micro solder balls. a) 96.5Sn-3.5Ag/ 60  $\mu\text{m}$  in diameter and b) 63Sn-37Pb/ 100  $\mu\text{m}$  in diameter.

Figure 1 shows SEM images of solder balls. In Figure 1-a), Sn-Ag balls of 60  $\mu\text{m}$  in diameter is shown and in Figure 1-b), Sn-Pb balls of 100  $\mu\text{m}$  in diameter is shown. In Figure 2, the size distributions are illustrated. Variations are less than  $\pm 3 \mu\text{m}$  and the precision of both the size and sphericity are very high. In Figure 3 the diameters measured on x and y directions of 50 balls (Left: Sn-Ag/ 60  $\mu\text{m}$ , Right: Pb-Sn/ 100  $\mu\text{m}$ ) are plotted. The tolerances of both sphericity and size are controlled within  $\pm 3 \mu\text{m}$ .

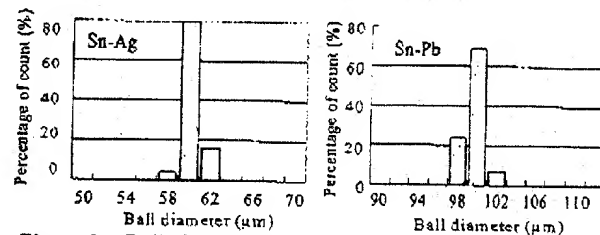


Figure 2a. Ball size distribution for Sn-Ag balls of 60  $\mu\text{m}$  in diameter (left) and Sn-Pb balls 100  $\mu\text{m}$  in diameter (right).

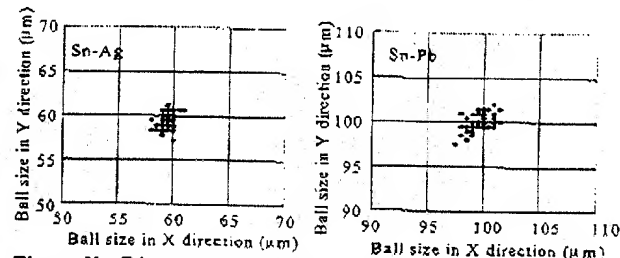


Figure 2b. Diameters measured in x and y directions for Sn-Ag balls of 60  $\mu\text{m}$  in diameter (left) and Sn-Pb balls of 100  $\mu\text{m}$  in diameter (right).

### Micro-Ball Arrangement Method

The balls are attached to the locations of the through-holes on one side of the arrangement plate by reducing the pressure in the other side so positioned as to match the points where bumps are to be formed. These balls are transferred to the points where electrode pads are located so that bumps are formed efficiently [6][7].

In Figure 3, the process flow of transferring and forming micro-ball bumps on the electrode pads is shown. For all micro-balls without any excess or shortage to be attached to the through-holes with the arrangement plate and retained in that position, it is necessary to make the micro-balls jump to a certain height by vibrating the ball container and bring the bonding head with the arrangement plate down and closer to the micro-balls. As shown in (1) of Figure 3, the micro-balls are retained in the through-holes (suction holes) by suction. As the diameter of the micro-balls becomes smaller, excess micro-balls tend to adhere to the portion other than the suction holes. Since the micro-ball's own weight is light, a suction leak occurs through an extremely small clearance between a normally attached ball and a suction hole, causing more than one micro-ball to adhere around one suction hole. Contamination and moisture content on the surfaces of the micro-balls also cause excess micro-balls to adhere to the arrangement plate. In order to remove these excess balls and continue retaining normally attached micro-balls in position, ultrasonic vibrations of the most appropriate vibration frequency and amplitude must be applied, as shown in (2) of Figure 3.

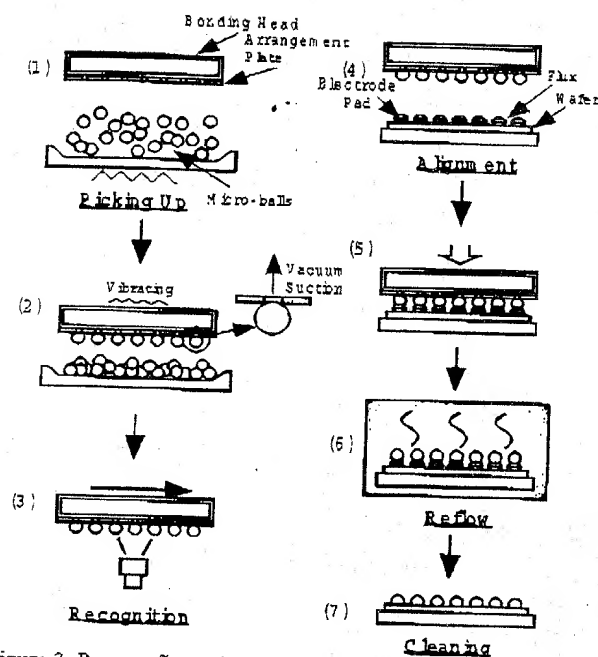


Figure 3. Process flow of micro-ball bumping

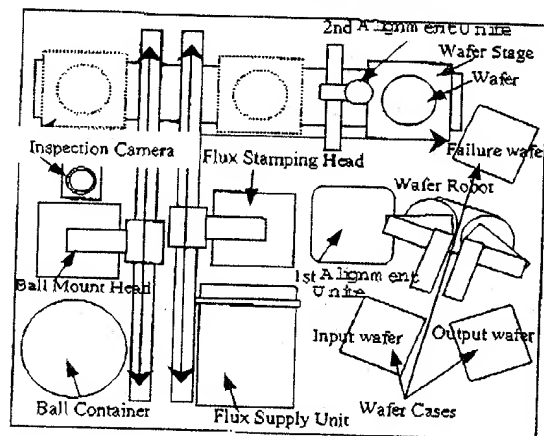


Figure 4. Schematic diagram of the micro-ball mounter.

A piezoelectric vibrator is operated to apply an ultrasonic vibration to the arrangement plate through the bonding head. Figure 5a and 5b show how excess micro-balls adhere to arrangement plate and the effect of applying ultrasonic (US) vibration. The micro-balls must then be viewed using an imaging processor to verify that the attached micro-balls are correctly arranged on the arrangement plate without any excess or shortage, as shown in (3) of Figure 3. If any of the micro-balls are incorrectly attached, those balls must be removed from the arrangement plate by using vacuuming nozzle. When it is verified by viewing the attached micro-balls that they are properly attached and aligned, the head moves to the bonding stage where the micro-balls are aligned to the

electrode pads on a wafer to which the micro-balls are to be transferred, as shown in (4) of Figure 3. As the last step of this process, the head is brought down and the micro-balls are touched to the electrode pads with a predefined load for transference, as shown in (5) of Figure 3. When the head is brought up, the pressure on the backside of the arrangement plate is increased above the atmospheric pressure to prevent the micro-balls from remaining on the through-holes of the arrangement plate. Before transferring micro-balls, the electrode pads are fluxed by stamping or screen printing. The micro-balls are retained in position of the electrode pads with the function of the adhesion strength of the flux. These temporarily retained micro-balls are heated to the temperature higher than their melting point in a furnace so that they are bonded to UBMs, as shown in (6) of Figure 3.

The authors have developed a unit capable of handling this entire process flow from steps (1) to (5) of Figure 3, fully automatically. Figure 4 shows a schematic diagram of a newly developed system which can be used for the wafer bumping of the size up to 8 inches. Wafers are loaded from a case using wafer robot. After detecting wafer position by alignment units, the wafer is moved to the fluxing stage, where flux is stamped on each electrode pads. The flux stamping plate has elastic bumps for transferring flux to the electrode pads. These elastic bumps are located at the same position as the electrode pads. After flux stamping, the wafer is moved to the ball mounting position. Then the micro-balls are transferred by the method as mentioned above. The machine cycle time is ca. 5 minutes.

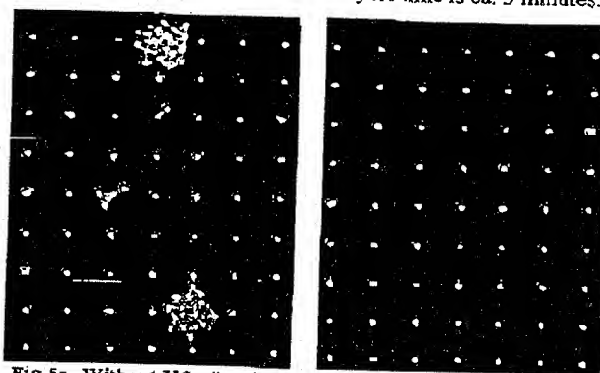


Fig. 5a. Without US vibration Fig. 5b. With US vibration

Figure 5. An example of excess micro-balls adhering to the arrangement plate (5a) and correctly attached (5b). Ball diameter: 100  $\mu\text{m}$ .

#### Formation of Solder Ball Bumps on the 8 inch wafers

Since the solder has poor wettability with the aluminum electrode pads, it is necessary to form the UBMs. Figure 6 shows a process flow to form solder bumps by transferring solder balls. The UBMs are deposited on the electrode pads on a wafer and the flux is supplied to these electrode pads by stamping. The amount of the flux to be transferred to the wafer could be controlled by squeezed gap of the flux supply unit.

In this experiment, Ni/Au UBMs are deposited by electroless plating. The method of electroless plating has the advantage in cost reduction of UBMs formation compared with the physical vapor deposition. To evaluate the bumps formed by the wafer level bumping system we prepared 8 inch test wafers. On Al electrode pads (size:  $100 \times 100 \mu\text{m}$ ), Ni of  $5 \mu\text{m}$  in thickness and Au of  $0.05 \mu\text{m}$  in thickness are deposited after zincate pretreatment. Solder balls are then transferred to the UBMs as described in Figure 6. The balls attached to the electrode pads on the wafer are melted and bonded to the electrode pads in a nitrogen atmosphere of reflow furnace, and the flux residue is removed by cleaning. The success rate of transferring the balls to the electrode pads is affected by the grade of ball diameter distribution and, therefore, it is necessary to use the ball with small size variation. An example of the ball with the irregular sphericity leading to transfer error is shown in Figure 8. These ellipse balls may cause choking through-holes of the arrangement plate.

In Figure 7, a picture of an 8 inch wafer with solder bumps and SEM image of solder bumps are shown. There are 619 chips in the wafer and 625 electrode pads per chip ( $25 \times 25$ ). Total number of pads is 385,000. Eutectic solder balls of  $100 \mu\text{m}$  in diameter are used, and electrode pads are set at a pitch of  $250 \mu\text{m}$ . The balls are positioned on the arrangement plate and transferred to the total pads on the wafer in one stroke. The success rate of ball transferring is obtained to be 99.995% or more. The pad positions of ball missing are repaired by a single ball mount equipment, resulting in the achievement of 100% yield in bumping. In the micro-ball bumping method excess balls can be easily removed before reflow process. In Figure 9, a cross section of these solder bumps is shown. There are no voids observed. The bump height and shear strength are measured, as shown in Figure 10 and 11 respectively. Five different positions are selected for the measurements as indicated in the drawing of the wafer in Fig. 10 and 11. The bump height is  $67.6 \pm 3.5 \mu\text{m}$  and the shear strength is  $56.23 \pm 7 \text{ gf}$ . When a shear test is conducted, fractures occurred only inside the solder bumps. Variation in the height is much smaller, compared with that in other bump formation methods. The Figure 12 shows the comparison of the bump height distribution between micro-ball bumping and screen-printing method. The average value of bump height is  $84.2 \mu\text{m}$  for micro-ball bumping and  $98.8 \mu\text{m}$  for screen-printing respectively. The difference of the average height is caused by the difference in pad size used and in solder volume. There is significant difference observed in the height distribution. The height variation in micro-ball bumping method is very small.

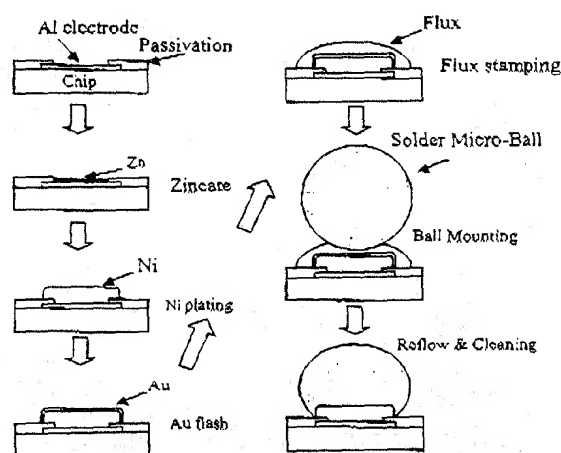


Figure 6. Process flow to form UBMs and solder bumps by micro-ball bumping.

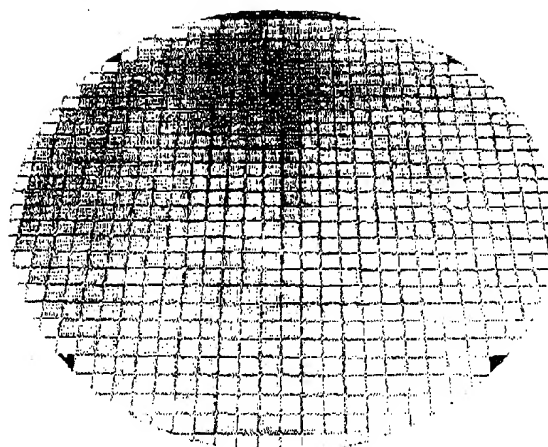
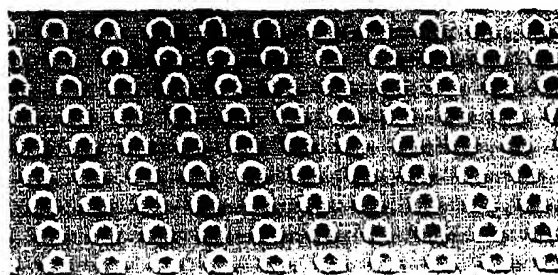


Figure 7. A picture of 8 inch wafer with solder bumps (lower) and SEM image of solder bumps (upper). (63Sn-37Pb solder balls of  $100 \mu\text{m}$  in diameter are used. Total number of bumps: 385,000).

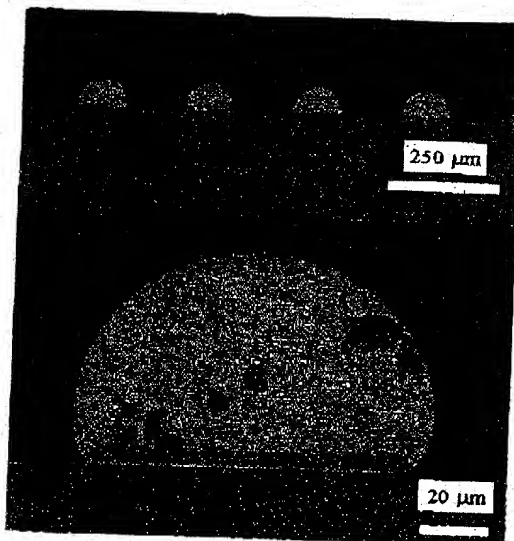


Figure 8. An example of irregular sphericity ball.

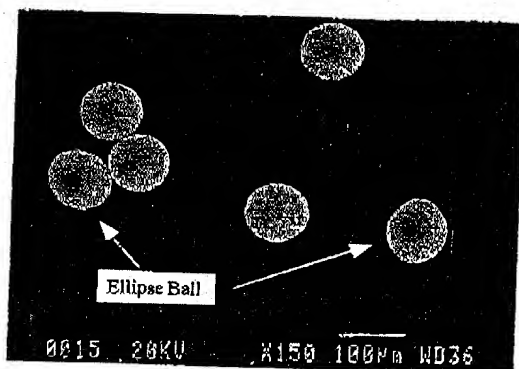
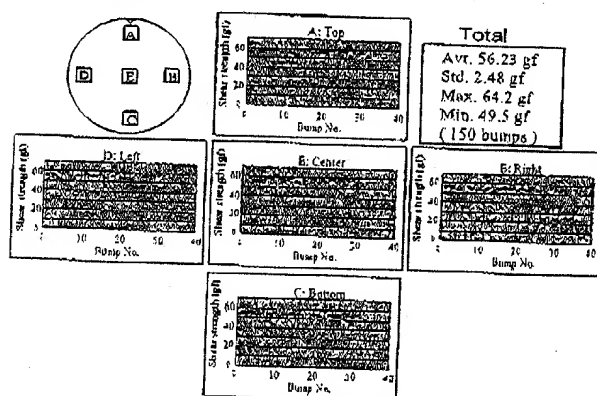
Figure 9. Cross sections of solder bumps formed using solder balls of 100  $\mu\text{m}$  in diameter on Ni / Au UBMs by electroless plating.

Figure 10. Height variation of micro-ball bumps in an 8 inch wafer.

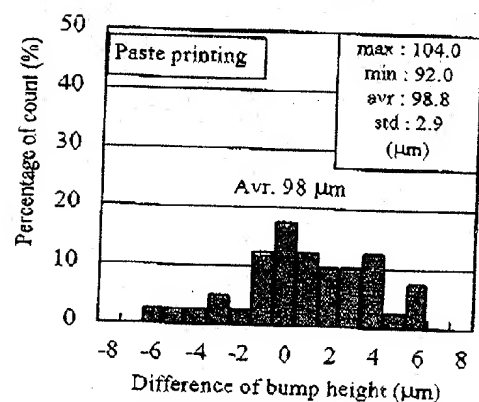
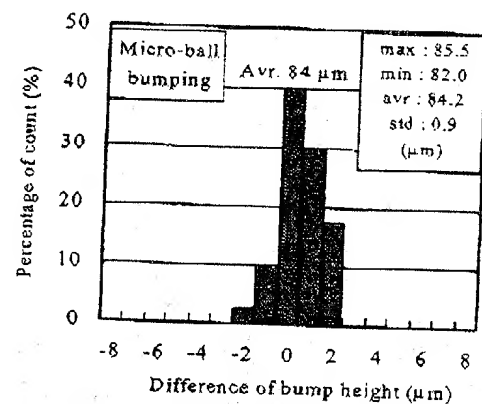


Figure 12b. Height variation of paste printing (bumps formed by printing paste).

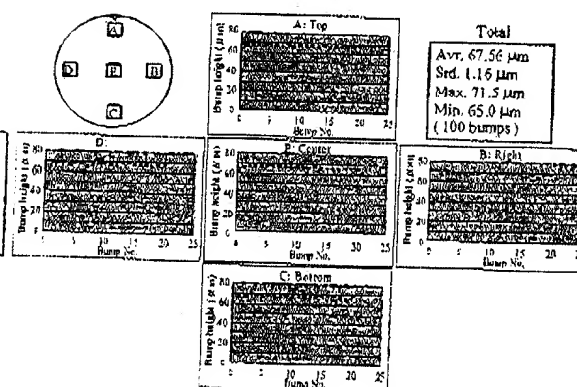


Figure 11. Shear strength variation of micro-ball bumps in an 8 inch wafer.

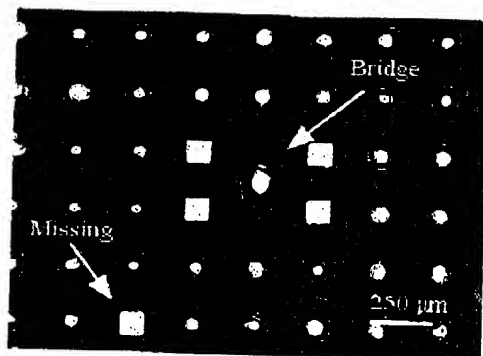


Figure 13. Typical failures of bumps after reflow (solder alloy: 63Sn-37Pb, ball diameter: 100  $\mu\text{m}$ ).

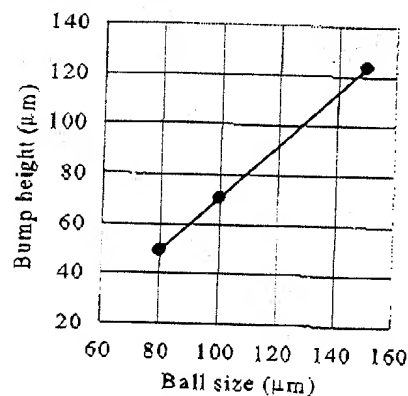


Figure 15. Bump height for the various ball sizes used (80, 100, and 150  $\mu\text{m}$ ). Electrode pad size: 110x110  $\mu\text{m}$ . 63Sn-37Pb solder balls were used.

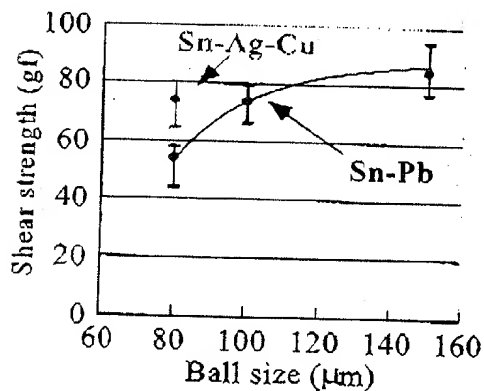
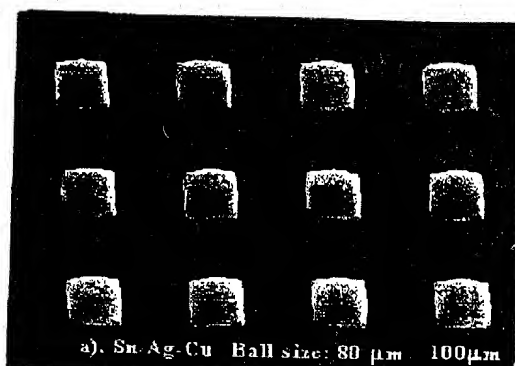
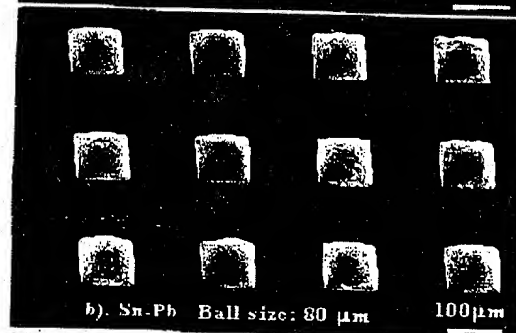


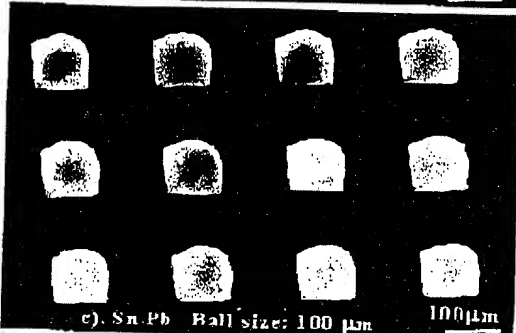
Figure 16. Shear strength of the various ball size (80, 100, and 150  $\mu\text{m}$ ). Electrode pad size: 110x110  $\mu\text{m}$ . 63Sn-37Pb solder balls were used.



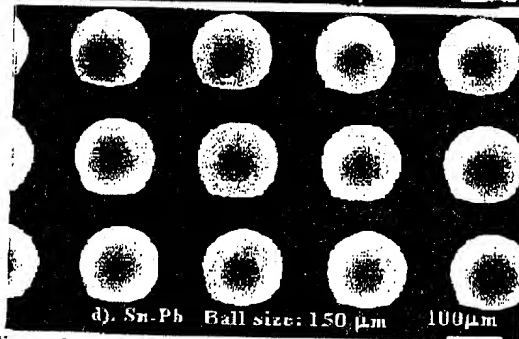
a). Sn-Ag-Cu Ball size: 80  $\mu\text{m}$  100 $\mu\text{m}$



b). Sn-Pb Ball size: 80  $\mu\text{m}$  100 $\mu\text{m}$



c). Sn-Pb Ball size: 100  $\mu\text{m}$  100 $\mu\text{m}$



d). Sn-Pb Ball size: 150  $\mu\text{m}$  100 $\mu\text{m}$

Figure 14. SEM images of bumps formed by using various balls. a) Sn-2.6Ag-0.6Cu/ 80  $\mu\text{m}$  in diameter, b) 63Sn-Pb/ 80  $\mu\text{m}$  in diameter, c) 63Sn-Pb/ 100  $\mu\text{m}$  in diameter, and d) 63Sn-Pb/ 150  $\mu\text{m}$  in diameter (electrode pad pitch: 250  $\mu\text{m}$ ).



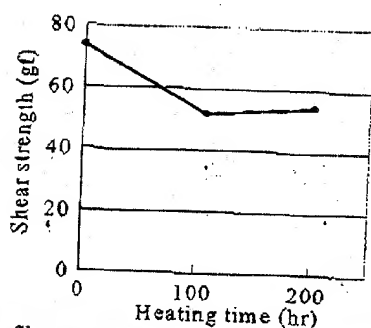


Figure 17a. Shear strength of solder bumps heated at 125°C.

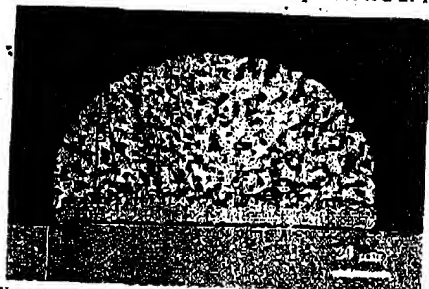


Figure 17b. A cross-section of a micro solder ball bump (heated at 125°C 108 hours).

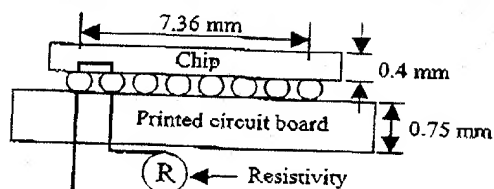


Figure 18a. A schematic diagram of Flip Chip bond for Thermal Cycle Test (Solder ball size: 300 μm).

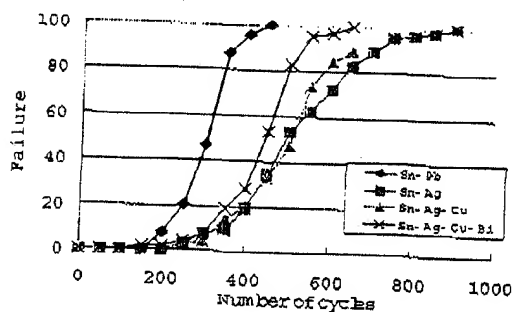


Figure 18b. The result of TCT using 300 μm solder balls (TCT condition: -40°C (20min)/ 125°C (20 min)).

Figure 13 shows typical failure patterns observed after reflow. Such problems as bump-to-bump bridging or ball missing could be resolved by optimizing the thickness and type of flux, or reflow conditions, ball transference conditions.

Figure 14 shows SEM images of bumps formed by using various size of 63Sn-37Pb and Sn-2.6Ag-0.6Cu balls from 80 μm to 150 μm in diameter. For all cases the same size of UBMs (110 μm x 110 μm) is used. The bump height increases with increasing ball size used as shown in Figure 15. There are no significant differences observed in bump shape as well as bump height between Sn-63Pb and Sn-2.6Ag-0.6Cu composition. Figure 16 shows the shear strength of bumps measured as reflowed depending on the ball size. The value of the shear strength for Sn-2.6Ag-0.6Cu alloy is markedly high compared with 63Sn-37Pb alloy. All bumps were sheared inside of the solder bumps.

A test of high temperature heating at 125°C for 200 hours is conducted on the bumps formed by using Sn-Pb balls of 100 μm in diameter. Shear strength of Sn-Pb bumps decreased slightly with heating at 125 °C for 108 hours. The decrease in shear strength is also observed by aging at room temperature after reflow in Sn-Pb bumps. The decrease appears to be related to the precipitation of Pb in Sn base phase. Figure 17b shows an optical micrograph of cross section of the bumps heated at 125°C for 108 hours. The value of the shear strength is kept to be almost constant for further heating.

Furthermore, the junction reliability of the FC bonding in Pb free materials is evaluated by TCT (Thermal Cycle Test). Figure 18a shows schematic diagram of test configuration. In order to clarify the effect of the material, test samples of FC bond are prepared without under-fill where the balls of 300 μm in diameter are used. The solder materials of Sn-3.5Ag, Sn-2.6Ag-0.6Cu, Sn-3Ag-0.75Cu-3Bi and 63Sn-37Pb are tested. A junction state is checked for the bumps of the outermost circumference of chip by resistivity measurement, and the failure number is counted. The samples are thermal cycled from -40°C to 125°C. A result is shown in Figure 18b. All three of Pb free materials are superior in fatigue resistance to 63Sn-37Pb solder.

This paper described wafer bumping method using micro-balls. This micro-ball bump method is also applicable to bumping on diced chips as well as substrate [5]. Figure 19 demonstrates an example of bumps formed on the PCB substrate, having electrode with 140 μm pitch.